physica status solidi (pss)

www.interscience.wiley.com

reprints

www.pss-rrl.com

www.pss-c.com

www.pss-b.com

www.pss-a.com

WILEY-VCH

REPRINT

Phys. Status Solidi C **7**, No. 3–4, 600–603 (2010) / **DOI** 10.1002/pssc.200982708

physica status solidi pss c
www.pss-c.com
current topics in solid state physics

Polycrystalline silicon thin films on glass obtained by nickel-induced crystallization of amorphous silicon

J. A. Schmidt*, N. Budini, R. D. Arce, and R. H. Buitrago

INTEC and FIQ, CONICET and UNL, Güemes 3450, S3000GLN Santa Fe, Argentina

Received 28 July 2009, revised 28 September 2009, accepted 28 October 2009
Published online 21 January 2010

PACS 64.70.dg, 68.55.A-, 81.10.Jt, 81.05.Cy, 81.15.Gh, 84.60.Jt

* Corresponding author: e-mail jschmidt@intec.unl.edu.ar, Phone: +54 342 455 9175, Fax: +54 342 455 0944

In this work, we use the nickel-induced crystallization process to crystallize a-Si:H thin films at temperatures compatible with the utilization of glass substrates. Hydrogenated amorphous silicon films are deposited on planar float glass (Schott AF37) by plasma-enhanced chemical vapour deposition. The films, between 400 and 1400 nm thick, are grown intrinsic, slightly p-doped (p^-) or with a combined structure of heavily p-doped / slightly p-doped (p^+/p^-) layers. On these films we sputter nickel with concentrations between 2.5×10^{14} and 3×10^{15} at./cm^2, and then we anneal the samples in a standard nitrogen-purged tube furnace. The process evolves through the formation of the nickel silicide $NiSi_2$, which has a lattice constant very similar to that of c-Si and acts as a nucleation centre. As a result of this thermal treatment we obtain thin polycrystalline films with a grain size over 100 µm. The high crystallinity of the samples is confirmed through optical and electron microscopy observations, X-rays diffraction and Raman spectroscopy.

© 2010 WILEY-VCH Verlag GmbH & Co. KGaA, Weinheim

1 Introduction Hydrogenated amorphous silicon (a-Si:H) can be deposited on glass substrates at low temperatures with a high deposition rate, giving uniform films even over large areas. However, despite many years of research, stability problems still limit the performance of a-Si:H-based devices and the electrical transport properties are worse than those of crystalline silicon (c-Si) [1]. Recently, renewed interest arose in using a-Si:H as a base material to obtain thin polycrystalline silicon (pc-Si) films on glass substrates. Having a grain size over 10 µm and an intra-grain quality comparable to that of c-Si, pc-Si is an attractive material to produce active-matrix liquid crystal displays, active-matrix organic light emitting diodes, and solar cells [2-5].

In an effort to reduce crystallization time and temperature, and to increase grain size, the effect of Nickel as an inductor of crystallization has been studied [2,3,6]. The addition of very small amounts of Ni (less than a monolayer) to the a-Si surface has a beneficial effect on crystallization. Although there is an agreement about the formation of the nickel silicide $NiSi_2$, which acts as a seed for the growth of crystalline silicon [7], the details of the crystallization mechanism are still under debate.

In this work, we explore the nickel-induced crystallization (NIC) of a-Si:H thin films deposited in a configuration suitable for the production of pc-Si solar cells. The proposed cell structure is glass/$p^+/p^-/n^+$/TCO, where p^+ is a heavily p-doped layer (back surface field), p^- is a slightly p-doped layer (base), n^+ is a heavily n-doped layer (emitter), and TCO is a transparent front contact.

2 Experimental details Samples were prepared on Schott AF-37 glass in a capacitively coupled Plasma Enhanced Chemical Vapour Deposition (PECVD) reactor. We used a relatively high frequency of 50 MHz and a power density of 120 mW/cm^2, being the distance between electrodes 1.1 cm. Intrinsic samples were prepared from pure silane (SiH_4), while diborane (B_2H_6) was added for p-type doping; in both cases without hydrogen dilution. The substrate temperature was 200 ºC and the gas pressure was 600 µbar, leading to a deposition speed of 15-20 Å/sec.

Three series of samples were deposited: A) intrinsic, with a thickness of 1000-1400 nm; B) p^- with a thickness of 600 nm, and C) p^+/p^- structures with thicknesses 80nm/320 nm. Nickel was deposited on top of the films by dc sputtering. The Ni concentration was determined on test

© 2010 WILEY-VCH Verlag GmbH & Co. KGaA, Weinheim

samples by atomic absorption spectroscopy [8], and varied between 2.5×10^{14} and 3×10^{15} atoms/cm^2. The samples were annealed in a furnace at atmospheric pressure under nitrogen flow. After a dehydrogenation step at 400 ºC, the samples were annealed for different time periods at 550-580 ºC.

Using the thin crystallized samples of series C as seed layers, we deposited an additional 1-µm-thick p^- a-Si:H layer on top of the p^+ / p^- structures. Then we annealed the resulting samples at 400 ºC for 24 h for dehydrogenation and at 570 ºC for crystallization. The aim of this annealing was to achieve a solid phase crystallization process, where the crystallizing a-Si cover layer copies the structure of the seed layer. The idea behind this process was to leave any possible metal contamination away from the p/n junction.

Crystallization was controlled through optical microscopy, scanning electron microscopy, X-rays diffraction and Raman spectroscopy. Raman spectra were taken using a Dilor spectrometer operating with the 632.8 nm line of a He-Ne laser. To assure that no local crystallization was induced by the laser, successive spectra were obtained to check for reproducibility.

3 Results and discussion

Figure 1 shows the Raman spectra of a series A sample at different stages of the crystallization process. The first spectrum from top corresponds to the as-deposited state; the broad peak at 480 cm^{-1} is evidence of the amorphous nature of this material. The sample was then covered with 1×10^{15} Ni atoms/cm^2 and dehydrogenated by annealing at 400 °C for 24 h. This intermediate dehydrogenation step is needed to avoid damage of the sample by explosive hydrogen exodiffusion. After further annealing at 580 °C for 6 h, the Raman spectrum shows evidence of incipient crystallization (second spectrum from top in Fig. 1). This is further confirmed by optical microscopy observations, as shown in Fig. 2a, where dispersed crystal nuclei can be seen.

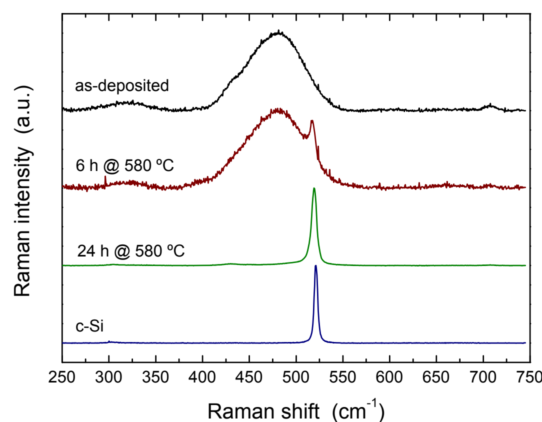

Figure 1 Raman spectra of an intrinsic sample at different stages of the crystallization process, and spectrum of crystalline silicon for comparison.

Further annealing of this sample allows the nuclei of Fig. 2a to grow, forming disk-shaped grains and straight grain boundaries when two grains collide. As can be seen in Fig. 2b for an annealing time of 18 h, there are grains with a diameter in excess of 120 µm. Additional annealing to a cumulative time of 24 h at 580 °C leads to a complete crystallization of the material, as shown in Fig. 2c (a Secco etching solution was used to reveal the grain boundaries).

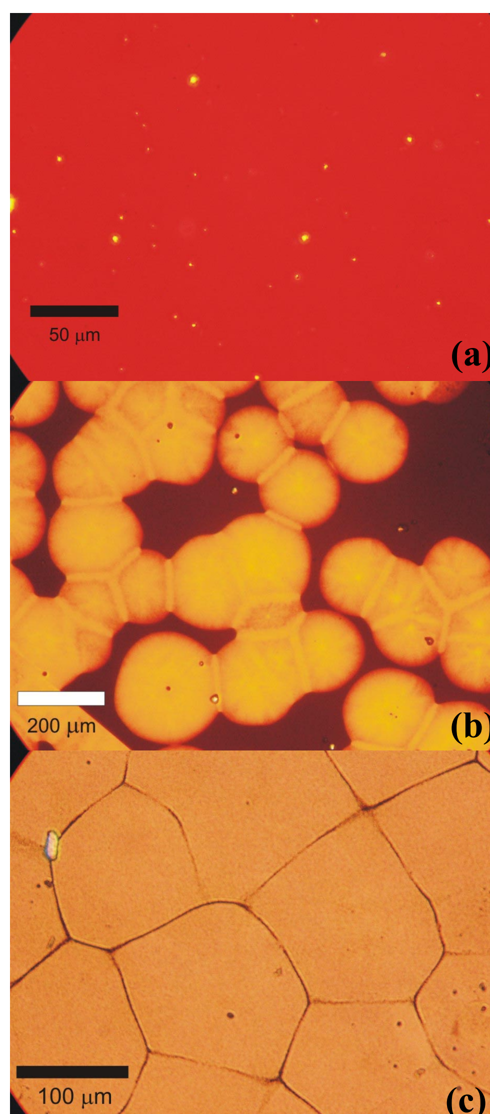

Figure 2 Optical microscope image in transmission mode of a Series A sample annealed at 580 °C for (a) 6 h; (b) 18 h; and (c) 24 h, Secco-etched to mark the grain boundaries.

The high crystallinity of this sample is also confirmed by the Raman spectrum of Fig. 1 (third spectrum from top), which is similar to that of a crystalline silicon wafer (bottom spectrum). Applying the usual formula to calculate the crystalline fraction [9], a value X_C = 89 % was obtained. Therefore, the amorphous or nanocrystalline contribution of the grain boundaries is still measurable. Moreover, the

 © 2010 WILEY-VCH Verlag GmbH & Co. KGaA, Weinheim

Raman peak of the crystallized sample is slightly wider than that of the crystalline wafer (FWHM of 6.65 cm^{-1} for the crystallized sample compared to 4.41 cm^{-1} for the crystalline wafer). This may be due to phonon dispersion caused by the inhomogeneous grain size [10]. Another possible explanation for the peak widening is the presence of an internal structure of the grains or of intra-grain defects.

The effect of nickel concentration on the final crystal size can be seen in Fig. 3 (squares). A maximum grain size of (126±20) μm has been found for a nickel concentration of 1×10^{15} Ni atoms/cm^2, with a decrease for both higher and lower concentrations. However, even for a Ni concentration of 2.5×10^{14} Ni atoms/cm^2 the grain size remains larger than 90 μm. These nickel concentrations are within the range of values used by other authors [2,3,11], and do not appear to be detrimental to the electrical transport properties. Minority carrier lifetimes as large as 19 μs have been measured for films with similar nickel concentrations, making them suitable for use as active photovoltaic layers [12].

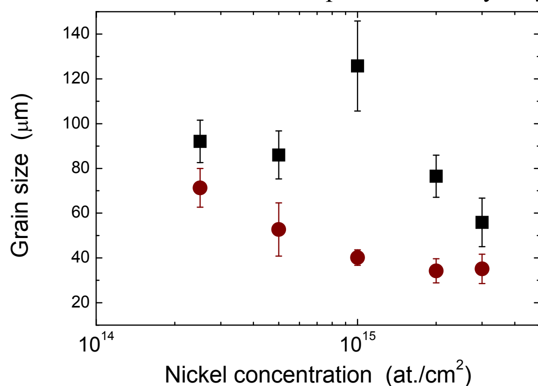

Figure 3 Final grain size as a function of nickel concentration sputtered on top of the intrinsic samples (squares) and the p^+/p^- structures (circles).

When the samples of series B where crystallized by the same procedure, we obtained essentially the same results as for samples of series A. This means that the low boron concentrations of the p^- layer – less than 10^{16} B at./cm^3 – do not affect the crystallization. Grain sizes in excess of 120 μm were also obtained on p^- samples for a Ni concentration of 10^{15} Ni atoms/cm^2.

On the other hand, the combined p^+ / p^- samples of series C do show a different behavior. Figure 4 is a picture of one of these samples, covered with 2.5×10^{14} Ni at./cm^2, and annealed at 550 °C for 24 h. Crystalline grains of ~70 μm, some of them still growing, can be seen. An internal structure of the grains can also be observed, with a cross-like shape. A second annealing at 570 °C for 24 h completely crystallized these samples. Figure 3 (circles) presents the final grain size as a function of the Ni concentration. One point to be noted is that the larger grain sizes are obtained for the lower Ni concentrations. The other point is that the overall grain size is smaller than in series A or series B samples. The internal structure of the grains and the lower grain sizes imply that the underlying p^+ layer is negatively influencing the crystallization of the p^- covering layer. The effect is probably due to the fact that high Boron concentrations promote the $NiSi_2$ nucleation. In intrinsic a-Si, $NiSi_2$ is usually formed at temperatures above 350 ºC. However, in heavily boron doped Si, Lu *et al.* [13] reported the formation of $NiSi_2$ at temperatures as low as 250 ºC. The substitutional nature of B makes the Ni atoms behave as more mobile interstitials, thus facilitating the silicide nucleation [14]. Finally, the larger density of crystalline nuclei leads to a lower grain size. The latter was confirmed by crystallizing a heavily Boron doped film, which resulted in a polycrystalline material with a grain size lower than 10 μm.

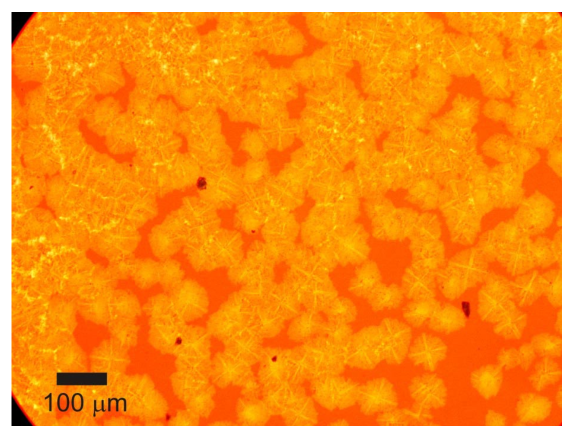

Figure 4 Optical microscope image in transmission mode of a glass/p^+/p^- structure, ~400 nm thick, annealed at 550 ºC for 24 h.

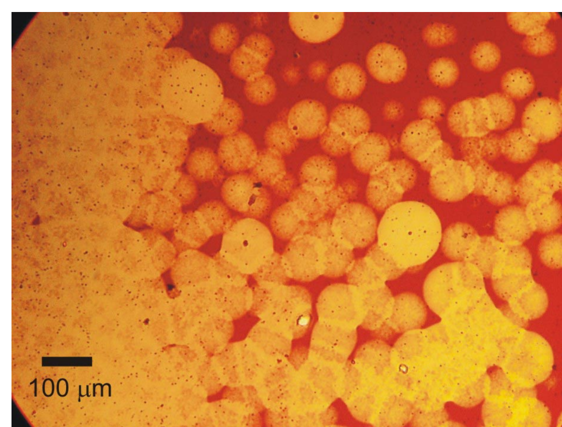

Figure 5 Optical microscope image in transmission mode of a 1-μm-thick p^- layer deposited on top of the glass/p^+/p^- structure of Fig. 4. The sample was annealed at 570 ºC for 24 h.

When these fully-crystallized glass/p^+/p^- structures were covered with an additional 1-μm-thick p^- a-Si:H layer, and then annealed at 570 °C for 24 h, the growth of disk-shaped grains resulted. This is shown in Fig. 5, where the

© 2010 WILEY-VCH Verlag GmbH & Co. KGaA, Weinheim

formation of straight grain boundaries when two grains collide can also be observed. The grains are larger than in the seed layer, being some of them larger than 100 μm in diameter. This result is quite surprising, since we were expecting an epitaxial growth from the grains of the seed layer. However, the grains of the covering layer appear to start growing from certain points of the seed layer. This may be an indication that there is a Ni accumulation at specific positions of the previously crystallized p^+/p^- samples. The issue of the final position of Ni after crystallization has been discussed in Ref. [15]. The two-dimensional distribution of Ni, obtained by time-of-flight secondary ion mass spectroscopy (TOF-SIMS) analysis, revealed a much higher concentration at the grain boundaries than inside the grains. The points with the highest concentration are those where three or more grain boundaries meet. Therefore, we argue that $NiSi_2$ precipitates at the grain boundaries of the seed layer act as inductors of the crystallization for the covering a-Si:H layer. These $NiSi_2$ precipitates start to move again, when the sample temperature is raised over 500 ºC [7]. Their lateral migrations in specific directions leave behind trails of c-Si with needle shape, as shown in [6] and [7]. The resulting growing front extends radially, leading to the formation of disk-shaped grains originating from a central $NiSi_2$ precipitate. The crystallization process is similar to that of the seed layer; only a small difference in the preferential orientation is observed. In the thinner films the disk-shaped grains are strongly (2 2 0) oriented, while in the thicker films the grains show a mixture of (2 2 0) and (1 1 1) plane orientations. Finally, the increase of the grain size in the second layer can be explained in terms of the lower Ni concentration available.

Figure 6 shows the fully crystallized glass/$p^+/p^-/p^-$ structure with a total thickness of 1400 nm and with grains larger than 80 μm. The addition of a heavily n-type (n^+) amorphous or microcrystalline layer to this structure would lead to a solar cell. The electrical characterization of these films will be presented in a future contribution.

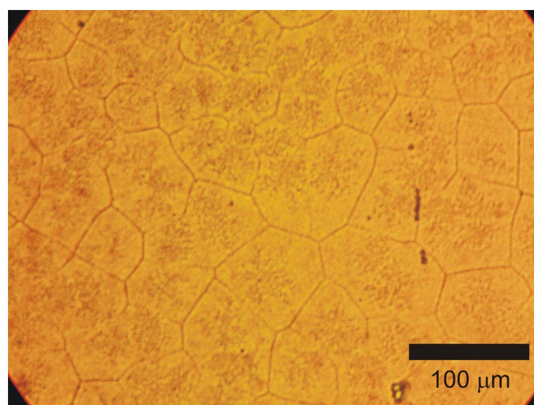

Figure 6 Optical microscope image in transmission mode of a fully crystallized 1-μm-thick p^- layer deposited on top of the glass/p^+/p^- structure of Fig. 4. The sample was annealed at 570 ºC for 48 h.

5 Conclusion

We have studied the nickel-induced-crystallization of intrinsic and boron doped a-Si:H samples. For intrinsic 1400-nm-thick samples, grain sizes in excess of 120 μm have been obtained, and the samples exhibit a high crystallinity. The same is true for slightly p-doped samples. On the other hand, heavily p-doped samples crystallize with a much lower grain size. To overcome this problem we have used p^+/p^- structures, which crystallize with grain sizes as large as 70 μm. If an additional p^- layer is deposited on top of these crystallized structures, we found that the growth is not epitaxial, but fully crystallized samples with a grain size larger than 80 μm can be obtained.

To get epitaxial growth from a Ni-induced crystallized seed layer, it might be necessary to remove the excess of Ni from the grain boundaries. This process would also help to reduce the Ni contamination that could negatively influence the transport properties of these films.

Acknowledgements This work was supported by ANPCyT (Projects 22-20267 and 22-25749), CONICET (Project PIP 5246) and UNL (Project CAI+D 28-158).

References

[1] C. R. Wronski, B. Von Roedern, and A. Kolodziej, Vacuum **82**, 1145 (2008).

[2] J. H. Choi, J. H. Cheon, S. K. Kim, and J. Jang, Displays **26**, 137 (2005).

[3] S-I. Maramatsu, Y. Minagawa, F. Oka, T. Sasaki, and Y. Yazawa, Sol. Energy Mater. Sol. Cells **74**, 275 (2002).

[4] A. H. Mahan, S. P. Ahrenkiel, R. E. I. Schropp, H. Li, and D. S. Ginley, Thin Solid Films **516**, 529 (2008).

[5] A. G. Aberle, Thin Solid Films **511/512**, 26 (2006).

[6] K. H. Kim, A. Nathan, and J. Jang, J. Non-Cryst. Solids **354,** 2341 (2008).

[7] C. Hayzelden and J. L. Batstone, J. Appl. Phys. **73**, 8279 (1993).

[8] M. B. Sperling and B. Welz, Atomic Absorption Spectrometry (Wiley-VCH, Weinheim, 1999).

[9] A. Gajović, D. Gracin, K. Juraić, J. Sancho-Parramon, and M. Čeh, Thin Solid Films **517**, 5453 (2009).

[10] S. B.Concari, R. H. Buitrago, Semic. Sci. Technol. **18**, 864 (2003).

[11] R. A. Puglisi, H. Tanabe, C. M. Chen, and H. A. Atwater, Mater. Sci. Eng. B **73,** 212 (2000).

[12] M. S. Mason, C. E. Richardson, H. A. Atwater, and R. K. Ahrenkiel, Thin Solid Films **501**, 288 (2006).

[13] S. W. Lu, C. W. Nieh, and L. J. Chen, Appl. Phys. Lett. **49**, 1770 (1986).

[14] J. D. Hwang, J. Y. Chang, and C. Y. Wu, Appl. Surf. Sci. **249**, 65 (2005).

[15] K. H. Kim, J. H. Oh, E. H. Kim, and J. Jang, J. Vac. Sci. Technol. A **22**, 2469 (2004).

© 2010 WILEY-VCH Verlag GmbH & Co. KGaA, Weinheim